Supporting Information

Alkaline-earth carbonate-supported Ru for quinoline hydrogenation: enhanced H_2 activation via electronic metal-support interaction

Yajing Han, [a] Pengfei Huang, [a] Xinkang Cui, [b] Quan Liu, [b] Qinggan Zeng, [b] Peixu Yang [*b] and Liqiang Wang [*b]

[a] College of Advanced Interdisciplinary Science and Technology (CAIST), Henan University of Technology, Zhengzhou 450001,

[b] School of Material Science and Engineering, Zhengzhou University, Zhengzhou, Henan 450001, P. R. China.

[*] Corresponding authors

Email addresses: yangpx@zzu.edu.cn (X. Yang); wangliqiang@zzu.edu.cn (L. Wang)

1. Methods

1.1 Materials

Anhydrous ruthenium(III) chloride ($RuCl_3$, 99.5%), quinoline and substituted quinolines (analytical grade), and alkaline-earth carbonates (e.g., $CaCO_3$ (99%), $MgCO_3$ (98%), and $BaCO_3$ (99%)) were purchased from Shanghai Aladdin Reagent Co., Ltd. Eggshells were obtained from a local supermarket. Commercial 5 wt% Ru/C (AR grade) was purchased from Shanghai Haohong Biomedical Technology Co., Ltd. Sodium borohydride ($NaBH_4$, 97%) was obtained from Tianjin Heowns Biochemical Technology Co., Ltd. Unless otherwise stated, all reagents were used as received without further purification.

1.2 Preparation of Catalysts

Preparation of RuNPs

To a $RuCl_3$ solution (1 mg mL^{-1}), $NaBH_4$ solution was added dropwise ($NaBH_4$:Ru in $RuCl_3$:2:1). After stirring for 3 h, the product was collected by centrifugation, washed with ethanol, and redispersed in ethanol for storage. The resulting sample was denoted as Ru NPs and was ultrasonicated for 5 min before use.

Preparation of $Ru/CaCO_3$

$Ru/CaCO_3$ was prepared by an impregnation method with a nominal Ru loading of ~0.5 wt%. Briefly, 1 g of $CaCO_3$ powder was dispersed in 15 mL of water and stirred for 30 min. 4.1 mL of $RuCl_3$ solution (5 mg mL^{-1}) was added dropwise, followed by stirring for 30 min. Subsequently, 0.2 g of $NaBH_4$ was dissolved in 10 mL of water and added dropwise to the above mixing solution; the mixture was stirred for 3 h. The solid was collected by filtration, washed with water, and dried under vacuum. The obtained solid was then calcined at 300 °C for 2 h under N_2 protection.

$Ru/MgCO_3$, $Ru/BaCO_3$, and Ru/EggShell were prepared using a similar procedure, except that the supports were replaced with $MgCO_3$, $BaCO_3$, and egg shell (ground into powder), respectively; all other conditions were the same.

1.3 Characterization

X-ray diffraction (XRD) patterns were recorded on a Bruker D8 diffractometer using Cu Kα radiation. Scanning electron microscopy (SEM) images were acquired on a Helios NanoLab 600i microscope. Transmission electron microscopy (TEM) was performed on an FEI Talos instrument operated at 200 kV. X-ray photoelectron spectroscopy (XPS) spectra were collected on a Thermo ESCALAB 250 equipped with Al Kα radiation. Metal loadings were quantified by inductively coupled plasma–optical emission spectroscopy (ICP–OES) using a Thermo ESCALAB 250Xi. N2 adsorption–desorption isotherms were measured at 77 K on a Micromeritics ASAP 2020 analyzer. Conversion and selectivity in nitro-compound hydrogenation were determined by HPLC (Shimadzu LC-20AD). H_2–D_2 isotopic exchange experiments were conducted as follows: For gas–liquid–solid three-phase hydrogen–deuterium exchange experiments conducted in a high-pressure reactor, the catalyst and substrate were loaded into the reactor, which was then sealed and purged with an inert gas to remove air. High-purity H_2 or D_2 was subsequently introduced to the desired pressure, and the reaction was initiated under constant-temperature stirring to ensure efficient gas–liquid–solid contact. Samples were collected at predetermined time points using an online sampling valve or after controlled depressurization. Kinetic profiles for H_2 and D_2 were constructed by plotting reaction conversion or product concentration as a function of time. The isotope effect was then evaluated by comparing the initial rates or steady-state values. The H_2-TPD experiment is carried out as follows. The catalyst is loaded into a quartz tube reactor and pretreated at 300°C under an inert gas flow for 50 minutes to remove surface impurities. After cooling to room temperature, a mixed Ar/H_2 gas is introduced for 1 hour to achieve saturated adsorption. Then, the system is switched back to an inert gas to remove physically adsorbed H_2. Finally, the temperature is linearly increased to 600°C at a constant heating rate, while the desorbed H_2 signal is continuously monitored using a thermal conductivity detector.

1.4 Hydrogenation performance evaluation

The chemoselective hydrogenation of quinoline was evaluated in a batch stainless-steel autoclave equipped with magnetic stirring. In a typical run, quinoline, catalyst, and solvent were charged into a 15 mL autoclave. Then the autoclave was purged with H_2 several times to remove air, and finally pressurized to 4 bar with H_2. The autoclave was placed in a heating mantle and maintained at 70 °C for 4 h with stirring at 800 r/min. After reaction, the reactor was cooled to room temperature and depressurized. After the reaction, the liquid phase was filtered and analyzed by HPLC.

Recycling tests were conducted by centrifugation to recover the catalyst from the reaction mixture, followed by three washing cycles with alternating water and ethanol, and vacuum drying. The recovered catalyst was reused under identical reaction conditions.

1.5 DFT calculation

The present first-principles calculations are performed using the projector augmented wave (PAW) method within DFT. The exchange functional is treated using the generalized gradient approximation (GGA) of Perdew-Burke-Ernzerhof (PBE) functional. The cut-off energy of the plane-wave basis is set to 400 eV for atom-optimization calculations. The vacuum spacing in a direction perpendicular to the plane of the catalyst is at least 15Å. The Brillouin zone integration is performed using 2 × 2 × 1 Monkhorst and Pack k-point sampling for surface structure. The self-consistent calculations apply a convergence energy threshold of 10−5 eV. The maximum Hellmann-Feynman force for each ionic optimization step is 0.05eV/Å.

2. Figures and Tables

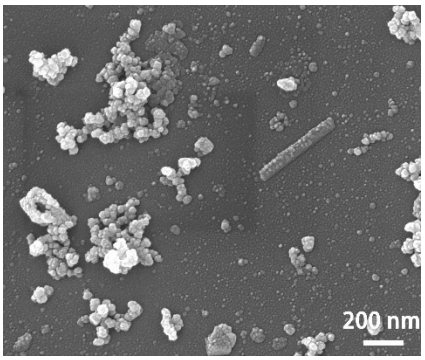

Fig. S1. Scanning electron microscopy (SEM) images of $Ru/CaCO_3$

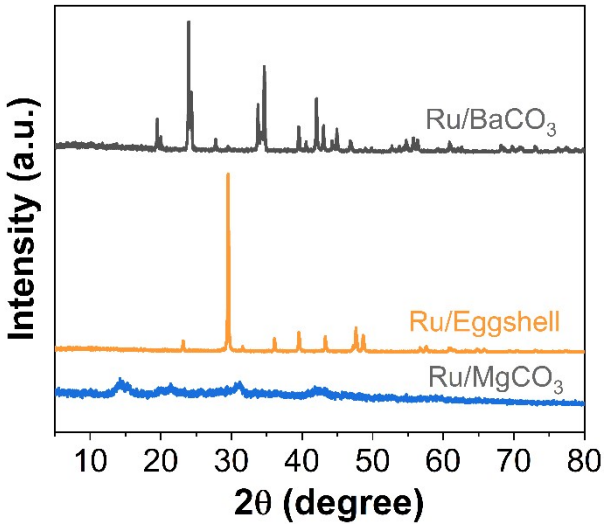

Fig. S2. XRD patterns of $Ru/MgCO_3$, $Ru/BaCO_3$, and Ru/eggshell.

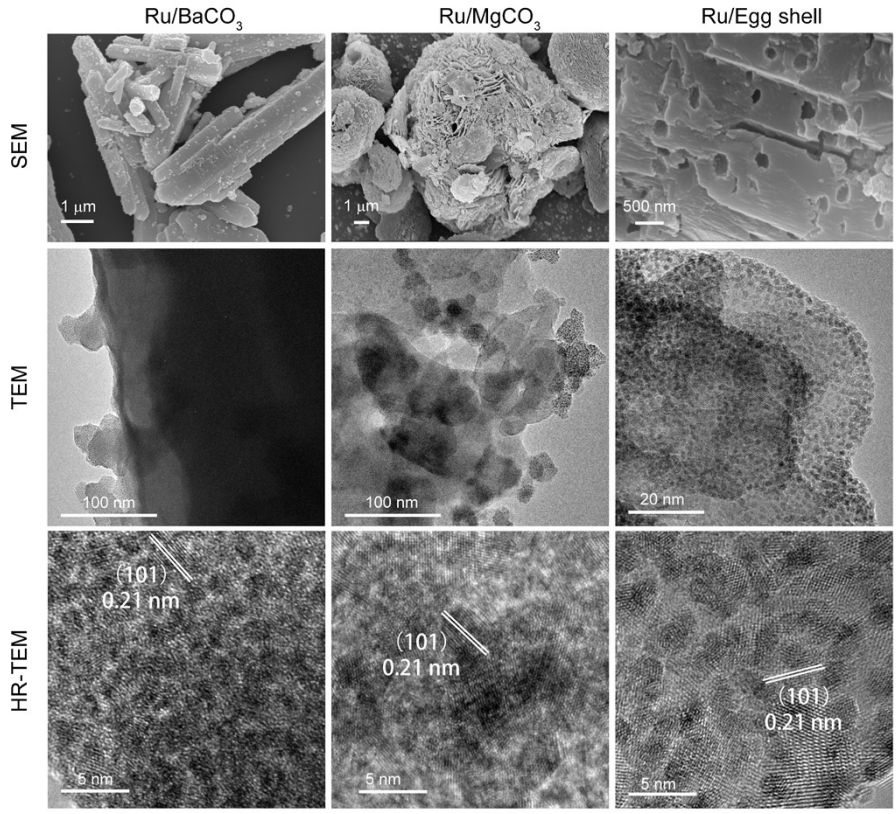

Fig. S3 SEM and TEM characterization of $Ru/MgCO_3$, $Ru/BaCO_3$, and Ru/eggshell.

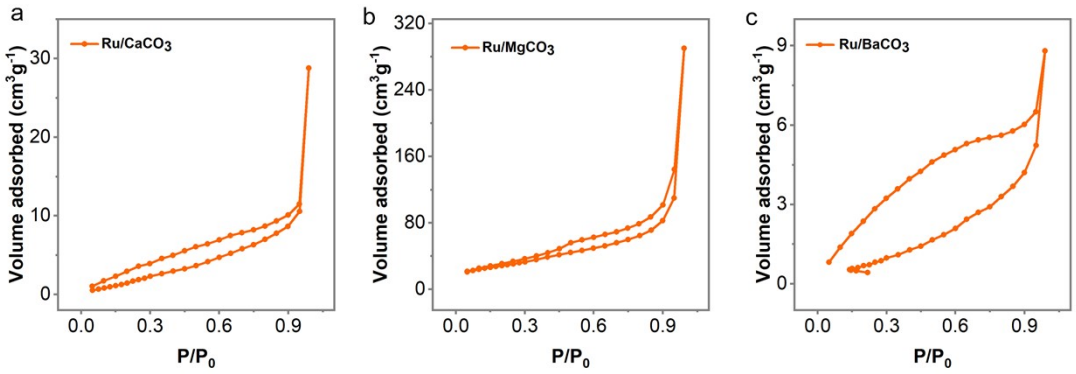

Fig.S4 N_2 adsorption-desorption isotherms of alkaline-earth carbonates supported Ru.

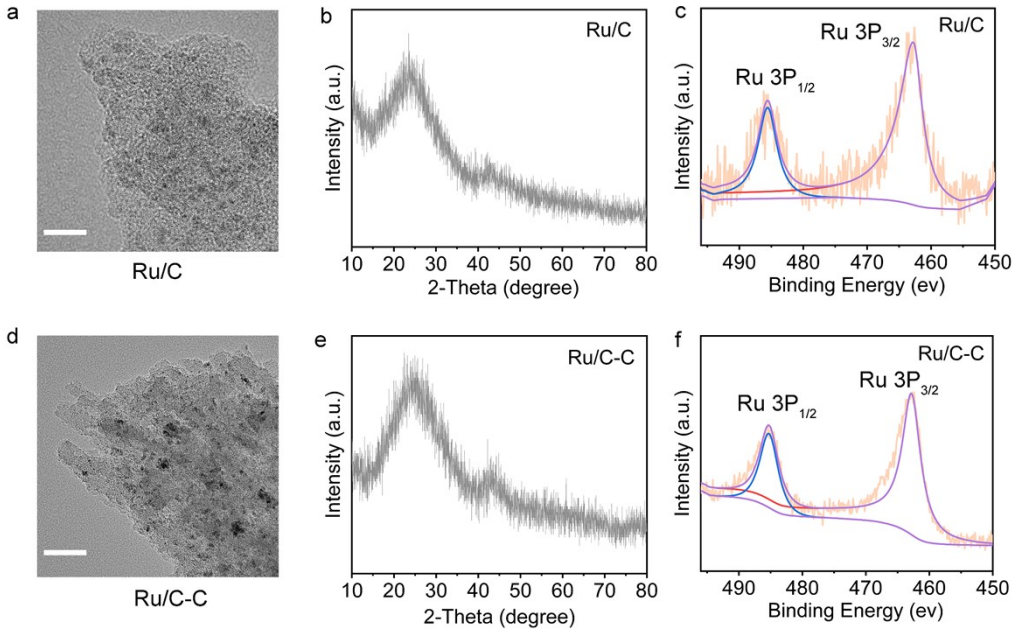

Fig. S5 (a,b) TEM images, (b,e)XRD patterns, and (c,f) Ru 3p spectrum of Ru/C (in-house made) and Ru/C-C (commercially available).

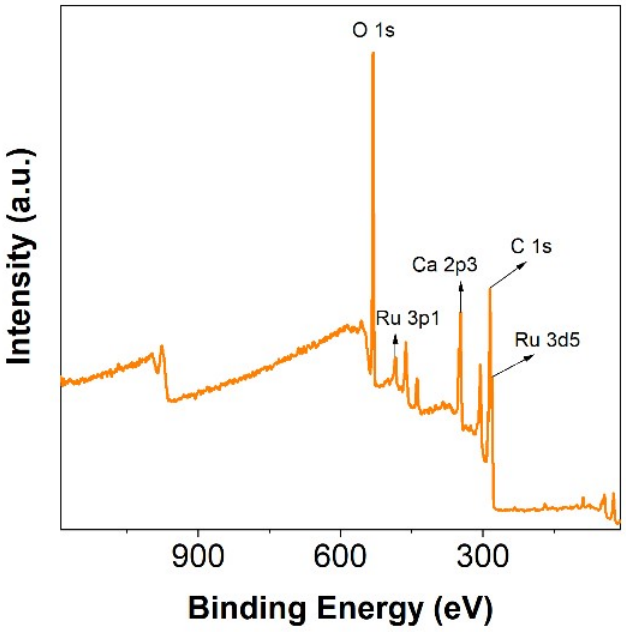

Fig. S6 XPS spectra of Ru/$CaCO_3$.

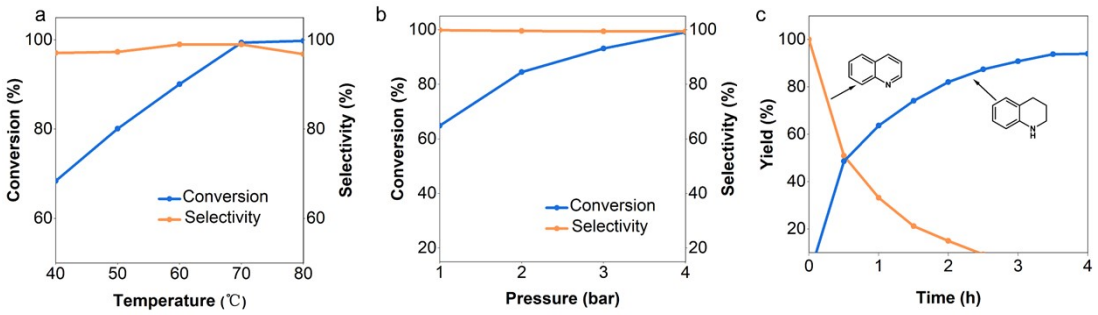

Fig. S7 Effects of (a) temperature, (b) H_2 pressure, and (c) reaction time on the conversion of quinoline and selectivity of 1,2,3,4-tetrahydroquinolines (THQs).

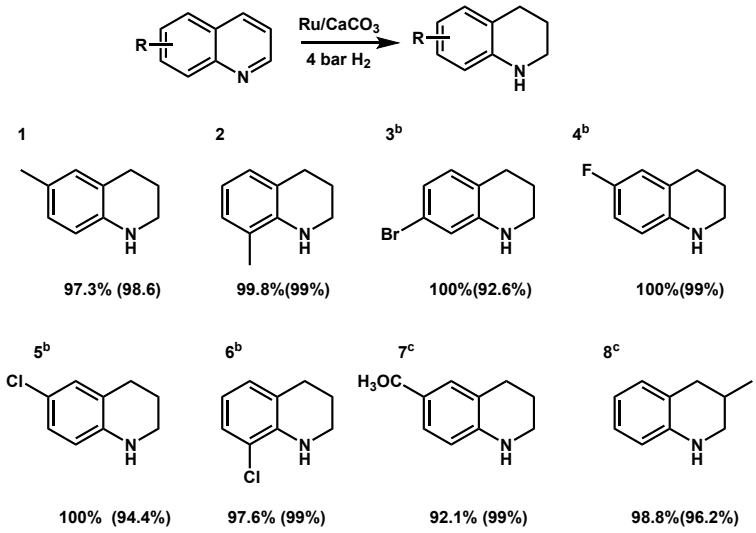

Fig. S8 Hydrogenation of various *N*-heteroarenes catalyzed by $Ru/CaCO_3$. Reaction conditions: 30 mg substrate with 20 mg $Ru/CaCO_3$, 4 mL solvent, 70 °C, 4 bar H_2, 4 h.

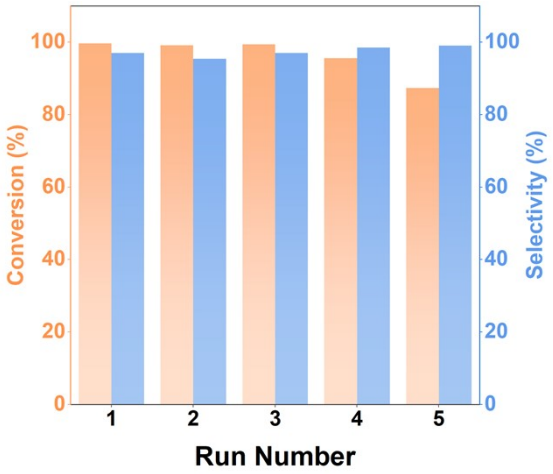

Fig. S9 Recycling experiment of $Ru/CaCO_3$

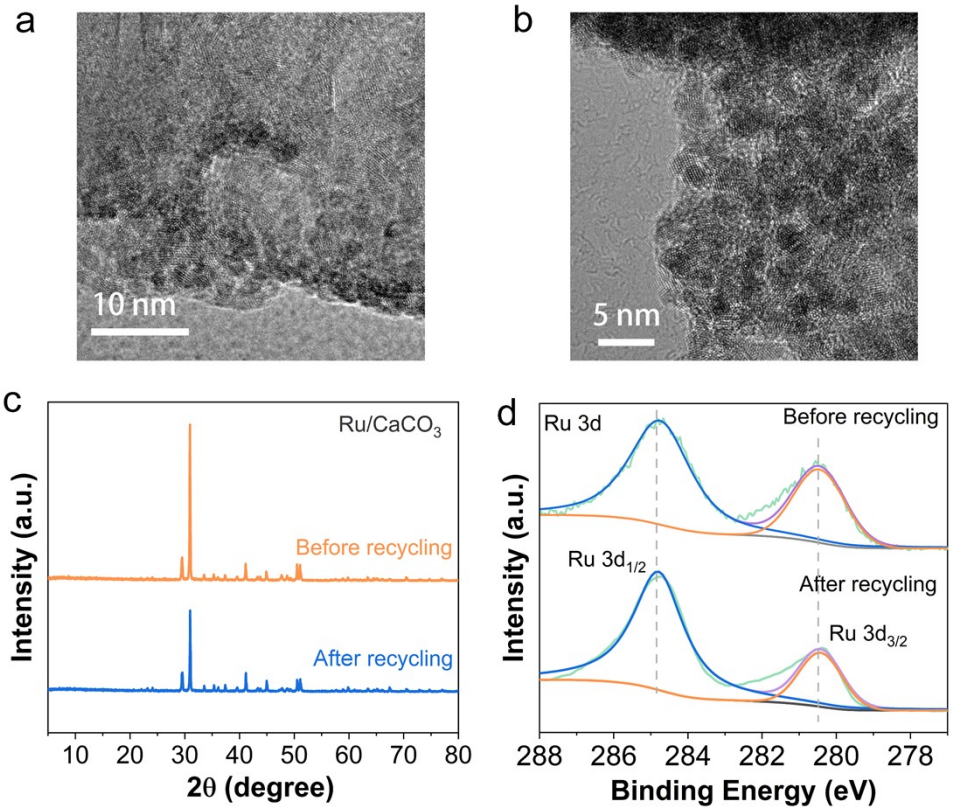

Fig. S10 Representative characterization of the reused $Ru/CaCO_3$: (a, b) TEM images, (c) XRD patterns, and (d) XPS spectra collected before and after five reaction cycles.

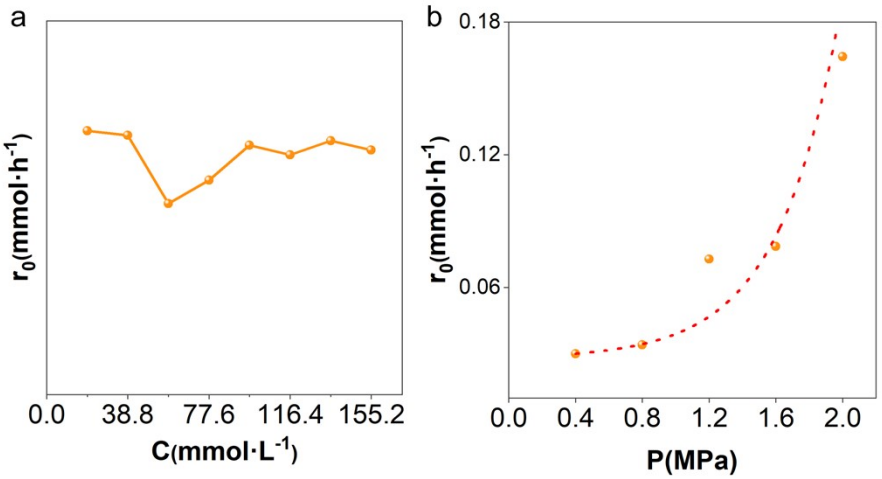

Fig. S11 (a) Influence of the concentration of quinoline (70 °C, 4 bar of H_2, 20 mg $Ru/CaCO_3$) and (b) the H_2 pressure (70 °C, 30 mg quinoline, and 20 mg $Ru/CaCO_3$) on the initial hydrogenation reaction rate.

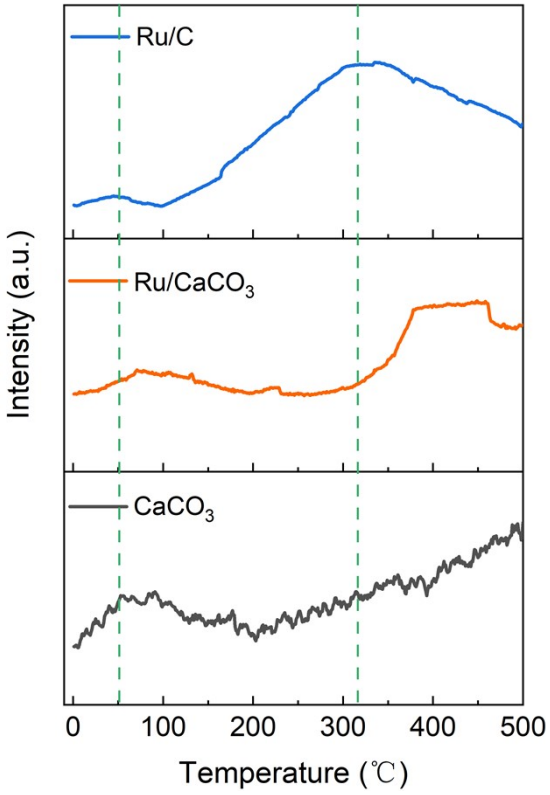

Fig. S12 CO_2-TPD of different supported Ru-based catalysts: CO_2 desorption below 100 °C is generally associated with physical adsorption, whereas the signals observed at 300–500 °C are typically attributed to chemically adsorbed CO_2. The $CaCO_3$-supported system exhibits a higher desorption temperature, suggesting stronger CO_2–surface interactions.

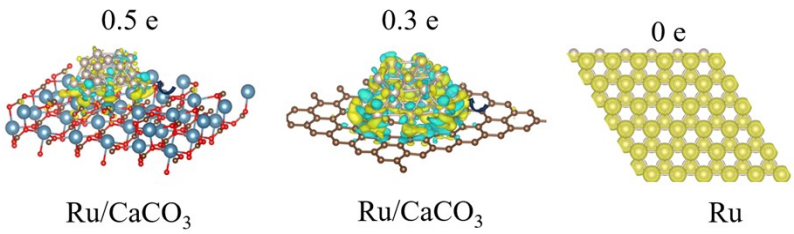

Fig. S13 charge-difference density of $Ru/CaCO_3$, Ru/C, and Ru.

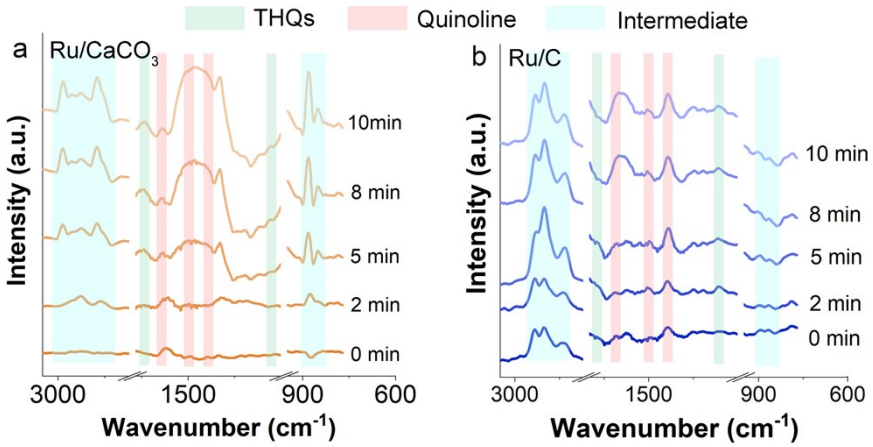

Fig. S14. In situ DRIFTS spectra of adsorbed quinoline on (a) $Ru/CaCO_3$ and (b) Ru/C as a function of time under flowing H_2.

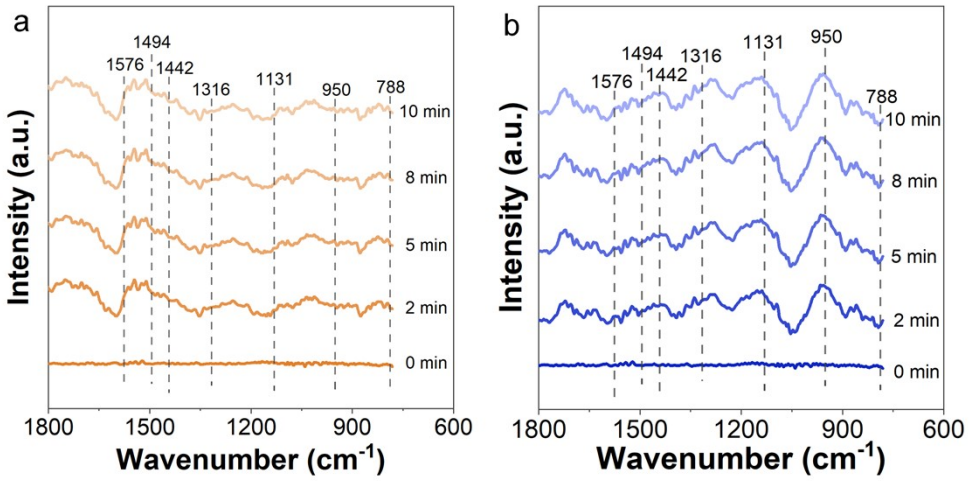

Fig. S15 Time-dependent quinoline adsorption on catalysts: (a) $CaCO_3$; (b) C.

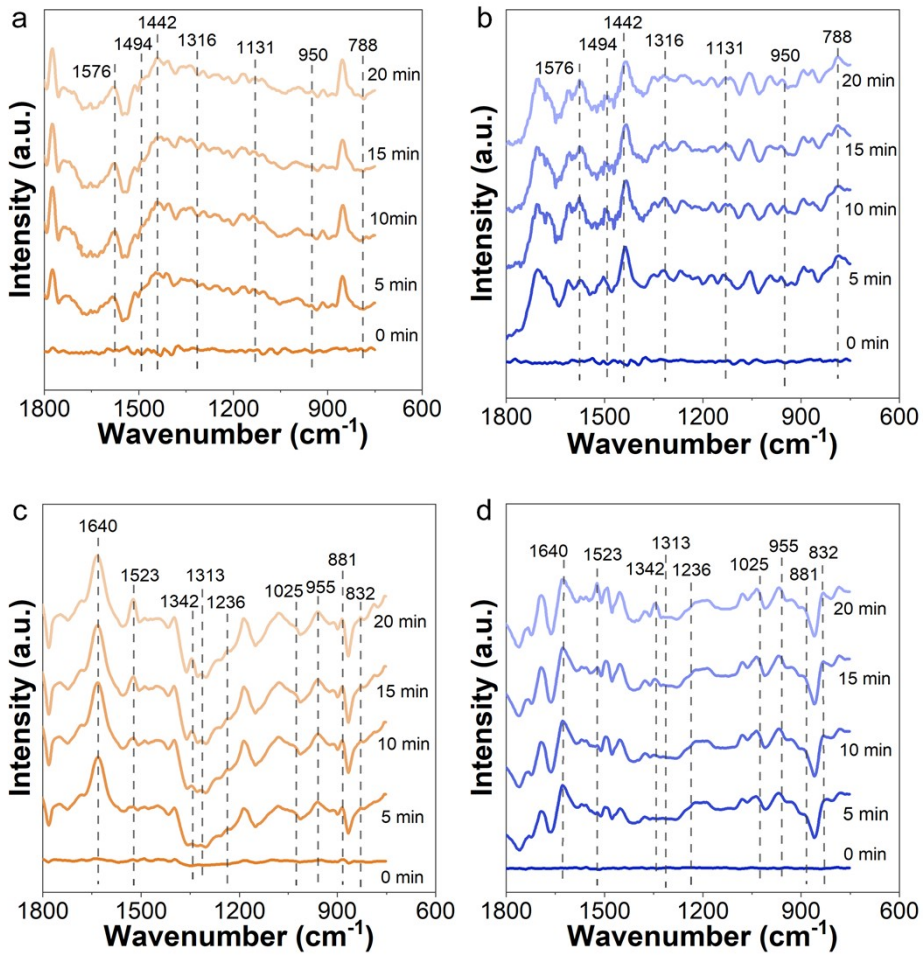

Fig. S16 Time-dependent quinoline adsorption on catalysts: (a) $Ru/CaCO_3$; (b) Ru/C, and THQs adsorption on catalysts: (c) $Ru/CaCO_3$; (d) Ru/C.

Table S1. Loading amounts of Ru in different catalysts determined by ICP-OES.

Catalyts	Element	Content(wt%)
$Ru/CaCO_3$	Ru	1.80
Ru/C	Ru	1.87
Ru/C-C	Ru	~5
$Ru/BaCO_3$	Ru	1.96
$Ru/MgCO_3$	Ru	1.98

Table S2. Comparison of the Catalytic Performance of Representative catalysts for quinoline hydrogenation.

Catalyst	H_2 (bar)	T (°C)	Time (h)	Con. (%)	Sel. (%)	Ref.
$Ru/CaCO_3$	4	70	4	99.9	99.9	This work
Ru/C	4	70	4	84.4	96.1	This work
Ru NPs	4	70	4	30.5	99.9	This work
$Ru/MgCO_3$	4	70	4	98.0	99.9	This work
$Ru/BaCO_3$	4	70	4	93.1	99.9	This work
$Pd/HS\text{-}NH_2$	20	100	-	92.6	99.9	Catal. Sci. Technol. 2017, 7, 2221.
Pd/CN	10	50	10	97.1	96.6	New J. Chem. 2018, 42, 16694.
Pd_{SA+NC}/TiC	20	60	6	99	99	Nano Lett. 2024, 24, 12666-12675.
Pd/NMC-X	4	40	2	99.9	99	ACS Appl. Nano Mater. 2024, 7, 22895.
Pd/PZs	1.5	40	4	98.9	98.5	Catalysts, 2024, 14, 345.
Pd/CN-1.0-A	4	30-60	1.5	99.9	99.9	Appl. Catal. A: Gen. 2025, 706, 120493.
PtRuNi/C	50	60	1	99.9	99.9	J. Alloys Compd. 2020, 834, 155203.
Pt/CeO_2	20	60	5	99	99	J.Catal. 2018, 359, 101.
PtNW	1	80	-	97.9	94.1	ChemCatChem 2013, 5, 2183.
$Pt_{AD}/C\text{-}Al_2O_3$	20	120	2.5	99.6	99.3	Chem. Eng. J. 2024, 481, 148706
PtMnAlNPore	8	120	12	92	100	J. Mater. Chem. A. 2025, 13, 11540.
$IL_{PEG1000\text{-}PF6}\text{-}Pt_{nano}$	30	130	1.5	99	99	J. Chem. Res. 2025, 49, 17475198241311697.
Rh NP	30	80	15-48	71	99	Angew. Chem. Int. Ed. 2016, 55, 292.
Rh/PEG4000	30	100	3	98	99	Appl. Catal. A: Gen. 2015, 499, 118.
$Rh_2O_3/SiO_2\text{-}C500$	5	50	0.6	99	99	Chem. Eng. J. 2025, 511, 162072
Ru/MgO	50	150	-	99.9	92	J. Catal. 2014, 311, 357.
Ru/NHPC	10	100	-	97	98	Green Chem. 2016, 18, 6082.
Ru/Al_2O_3	70	160	2	100	99.1	RSC Adv. 2020, 10, 11039.
Ru/CuC	20	80	2	99.6	99.9	Nano Research 2016, 9, 2632.
$Au_{0.9}Pd_{0.1}/CNR$	20	100	-	92.6	99.9	J. Mater. Chem. A 2017, 5, 25314.
$Au/HAS\text{-}TiO_2$	20	60	3	100	100	J. Am. Chem. Soc. 2012, 134, 17592.
Ir/α-MoC	30	120	1	81	99	Natl. Sci. Rev.2022, 9.

Table S3. Effect of solvents on the selective hydrogenation of quinoline using $Ru/CaCO_3$.

Entry[a]	Solvent	Con. (%)	Sel. (%)
1	Water	99.4	99.9
2	MeOH	2.7	97.3
3	EtOH	39.6	98.1
4	Isopropanol	2.8	96.8
5	THF	11.0	91.2
6	MeCN	1.1	98.9
7	1,4-Dioxane	6.5	97.8

[a] Reaction conditions: 30 mg substrate, 20 mg $Ru/CaCO_3$, 4 mL solvent, 70 ℃, 4 bar H_2, 4 h, 800 r/min.